Electrical and Thermal Properties of NiCd Battery for Low Earth Orbit Satellite's Applications

M. ZAHRAN[1,2] & A. ATEF[2]

1 Electronics Research Institute, NRC Blg., El-tahrir St., Dokki, 12311-Giza, EGYPT
+202(3310512/3351631), _____ _____

2 National Authority for Remote Sensing and Space Science, Space Department,
23 Josef Teto St., Nozha, Cairo Egypt. Tel./Fax. +2020-6225821/6225833.

Abstract: Nickel-Cadmium (NiCd) batteries are well proven for LEO satellite's application. NiCd batteries are not very energy-dense, but they are inexpensive, lightweight, and extensively proven [1].

This paper describes the development of a simulation electrical and thermal model for a sealed rechargeable NiCd battery. Based on the concept of this battery type, a mathematical description of the various electrochemical and thermal processes occurring inside the battery can be given. A family of curves was introduced as a result of the modelling and simulation work in this paper. Some of these curves are verified with an experimental work results. The validation phases and the dynamics of the battery parameters convergence are extremely high and acceptable. The electrical and thermal properties are shown.

One aim of the present research is to study the thermal behavior of a NiCd battery for space applications. After a description of the effect of temperature on NiCd cell electrical properties, a thermal model has been developed to calculate the temperature profile in a NiCd cell stack during charging and discharging processes during ground testing. The equations describing the temperature distribution of the cell stack are derived and then the temperature results are presented. Finally, the calculated temperatures are compared to those measured during ground testing.

When selecting batteries for space flight applications, the following requirements should be considered: ampere-hour capacity, recharge-ability, depth of discharge (DOD), lifetime, temperature environments, ruggedness, and weight. Many batteries have been qualified and used for space flight, enhancing the ease of selecting the right battery.

Key Words: Microsatellite, Storage Subsystem, NiCd Batteries, Modelling and Simulation

1. Introduction

Most satellites use storage batteries (NiCd, NiH_2, usually) to store excess energy generated by the solar arrays during periods of exposure to the Sun. During eclipse, the batteries are used to provide power for the satellite subsystems. The batteries are recharged when the satellite exits the eclipse [2].

Batteries shall be designed to support the spacecraft through the launch sequence, including all anticipated contingencies and through all foreseen losses of solar energy during the mission, including those resulting from failures (e.g. de-pointing due to loss of pointing sensors, attitude control). Almost all battery technologies used aboard spacecraft can be hazardous if not properly managed. Most are capable of delivering very high currents when shorted. When abused, cells can develop excessive internal pressure and in extreme cases explosively [3]. Study of the battery performance based on the experimental work is costly and not available for designer especially during the preliminary design phases. The mathematical modelling and simulation help the designer to study and analyze the performance of the battery stack during the design phases.

The goal of a battery charging system is to provide a maximum recharge to a battery without overcharging it. Overcharging a battery, especially at relatively high currents, will dramatically shorten its lifetime and its charge capacity and may cause physical damage to the battery and its surroundings. Most charging systems stop charge based on the voltage of a battery to a constant current charge. NiCd battery, which is one of the most common batteries, used for LEO satellite produce a repeatable characteristics voltage profile under a constant current charge that makes it relatively simple for the charging system to detect the moment of peak charge. However, most of LEO satellites do not have a stable power source and standard power budget that is capable of supplying a constant current during battery charging, so the characteristics of voltage profile is altered, and then a voltage termination system can't perform well.

The temperature of a battery under charge is another important parameter that should be used to control the charge process of NiCd batteries. As the

battery reaches full charge, the internal cell temperature rises dramatically because of gassing generation at end of charge that acts to increase to pressure in a constant volume container of battery jar. Detecting this temperature can be used as an effective assistant parameter of terminating charge to a battery.

In NiCd cells, it is a result of the charge in the electrochemistry from an uncharged state to a charged state that causes the subtle decrease in temperature. The temperature of the cell remains relatively constant during a large portion of the charge cycle because most of the applied current is charging the active materials at plates and very little goes into gas-generation reactions. At time continues, the battery finds it increasingly difficult to convert uncharged materials into charged materials as the uncharged materials rapidly disappears. The impedance of the battery begins to rise and soon it becomes easier to break down the electrolyte than to convert inactive materials to a charged state. At this point, the chemical reaction begins a transition from an endothermic reaction to an exothermic reaction that gives off heat and causes a rapid increase in temperature. This change in the chemical reaction inside the battery marks the onset of the overcharge region. A large amount of gas is created as both pressure and then temperature build. The battery can accept some additional energy before charge should be stopped, however the battery is sending signals that it is nearing the end its ability to take much more. This phenomenon describes the curve of upper knee of the battery voltage profile at end of charging region. So the battery charging system should stop charging before reaching this state [4].

Battery is composed of one or more cells, either parallel or series connected to obtain a required current/voltage capability (batteries comprised of series connected cells are by far the most common).

The battery stack under study is a NiCd battery consists of 22 series cells where the nominal capacity of each is 8Ah [5].

2. Chemistry of NiCd Batteries

Both Juengner and Edison contributed significantly to the development of the NiCd battery [6]. In a NiCd cell, the charge–discharge reactions at the nickel positive electrode (cathode) and Cadmium negative electrode (anode) of the NiCd cell are described in [4] as follows:

2.1. Positive electrode

In a NiCd cell, the charge–discharge reactions at the nickel positive electrode (cathode) proceed via homogeneous solid-state mechanism through proton transfer between nickelous hydroxide (discharged active material) and nickelic hydroxide (charged active material). The charge–discharge reactions of the nickel electrode have been expressed as:

$$NiO_2 + 2H_2O + 2e^- \underset{Charge}{\overset{Discharge}{\rightleftharpoons}} Ni(OH)_2 + 2OH^-$$

$$(E^0 = 0.49V) \quad (1)$$

In Eq. (1), NiO_2 forms the active material of the positive plate with $Ni(OH)_2$ as the discharged product which is reconstituted as NiO_2 during recharge.

2.2. Negative electrode

Cadmium hydroxide is the discharged active material at the negative electrode (anode) of the NiCd cell. During charge, cadmium hydroxide at the negative electrode is converted to metallic cadmium via a dissolved complex intermediate product as described below.

$$Cd(OH)_2 + OH^- \longrightarrow Cd(OH)_3^-$$

$$Cd(OH)_3^- + 2e^- \longrightarrow Cd + 3OH^-$$

The overall cell reaction at the negative electrode is:

$$Cd + 2OH^- \underset{Charge}{\overset{Discharge}{\rightleftharpoons}} Cd(OH)_2 + 2e^- \quad (2)$$

$$(E^0 = -0.81V)$$

2.3. NiCd Cell overall reaction

Accordingly to the positive and negative electrodes reactions, the overall cell reaction can be given as follows:

$$2NiOOH + Cd + 2H_2O \underset{Charge}{\overset{Discharge}{\rightleftharpoons}} 2Ni(OH)_2 + Cd(OH)_2$$

$$(E_{cell} = 1.3V) \quad (3)$$

To ensure proper functioning of the sealed NiCd cell under a variety of operating conditions, it is designed to be positive-limited. This insures that only O2 evolution occurs under normal operating conditions which diffuses to the cadmium electrode and combines with active cadmium to form Cd(OH)2 according to the reaction.

$$Cd + \tfrac{1}{2}O_2 \longrightarrow Cd(OH)_2$$

$Cd(OH)_2$ is converted to active Cd according to reaction (1) during the cell charge. The negative to positive plate capacity ratio usually varies between 1.5 and 2. The discharge reserve is typically between 15 and 20% of positive capacity and the charge reserve or overcharge protection is about 30% of positive capacity. Under deep-discharge conditions, due to inevitable differences in storage capacities of series connected cells in the battery, H2 evolution may occur at the positive electrode which is consumed at a very low rate at the positive electrode. Hence, repeated occurrence of overdischarge may cause internal pressure build-up leading to cell burst. The operating principle of a sealed NiCd cell is depicted in Fig. 1.

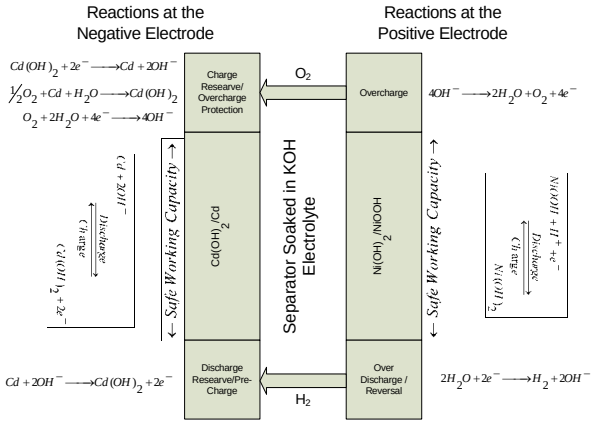

Fig. 1, Operating principle of a sealed NiCd cell

The performance of NiCd cells depends on several factors such as cell type, cell construction, manufacturing process and operating temperature, charge–discharge rates, previous history of the cell, length of open-circuit stand, age of the cells, etc. Fig. 2 Charge voltage profiles for different types of NiCd battery at C/10 rate;

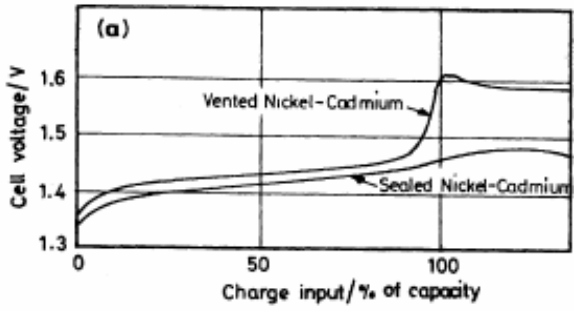

Fig. 2, Vented and Sealed NiCd Cells Voltage Capacity curves.

3. Operation characteristics of NiCd battery

3.1. Reliability of NiCd batteries

Sustained high-current overcharge and cell polarity reversal (during discharge) are the main killers of NiCd battery [7]:

- If a high charge rate is used, it is essential to terminate charge when the cell is full. If this is not done, the temperature and pressure within the cell will rise quickly as the charging current is dissipated as heat.
- Avoiding abusive high-current overcharge can only be ensured with a well-designed charging system that responds to the signal the battery gives when fully charged.
- Cell polarity reversal is a potential problem with any series-connected string of cells: as the battery is discharged, the cell that goes down to zero volts first will continue to have current forced through it by the other cells. When this occurs, the voltage across the fully discharged cell is reversed.
- A cell that has current forced through it with a reverse voltage across it will heat up very quickly and vent gas in a similar mode to that described for the sustained overcharge, with the same resultant damage.

3.2. Age-Related Failure Modes

After a period of time, the insulator within a NiCd battery often develops holes which allow the cell to grow crystalline "shorts" that provide a conduction path between the positive and negative electrodes of the cell (which basically shorts out the cell). If this happens, you may have to blow open this short with a high current pulse before the cell will again accept charge (a process sometimes referred to as "zapping"). A leaky NiCd cell will always have a high self-discharge rate and will re-grow internal shorts if left on the shelf without some kind of trickle charge [7].

3.3. Memory affect of NiCd batteries

NiCd batteries are known to have a memory effect. i.e. if the battery has been repeatedly discharges slightly (10-20%) and then recharged again, it will gradually develop a memory effect and loss some of its capacity after a period of time.[8]. The memory effect is reflected as a step in the discharge curve of a cell shown in Fig. 3.

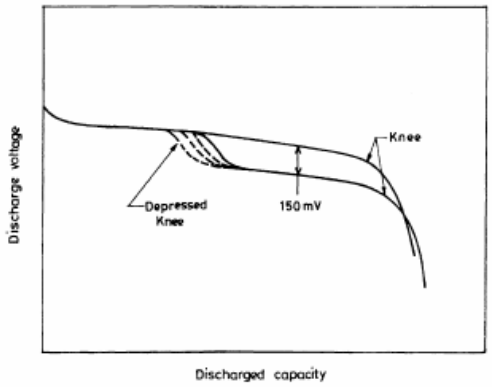

Fig. 3, Memory effect of NiCd Batteries on the discharge voltage curve.

This is mainly observed in hermetically sealed aerospace NiCd cells and does not occur normally during commercial use. But, in practice, the memory effect cannot exist (a) if the cells are charged to 100% of their actual capacity, (b) if the cells are discharged to variable depth in each cycle, and (c) if the cells are discharged below 1 V. Such capacity loss can be recovered by performing a number of deep discharge and charge cycles [6].

3.4. Internal resistance

The internal resistance of NiCd cells dependent on several factors; including ohmic resistance (due to conductivity, the structure of the current collector, the electrode plates, separator, electrolyte or other features of the cell and battery design), resistance due to activation and concentration polarization, and capacitive reactance. In most cases the effects of capacitive reactance can be ignored. Polarization effects are dependant in a complicated way on current, temperature, and negligible for pulses of short duration, that is less than a few milliseconds.

The NiCd cell is noted for its low internal resistance due to the use of thin and large surface area plates with good electrical conductivity, a thin separator with good electrolyte retention, and an electrolyte having a high ionic conductivity. During discharge, the activation and concentration polarization are negligible, at least at low and moderate rates, and the internal resistance of the cell, and the discharge voltage, remains relatively constant from the state of full charge to the point where almost 90% of the cell's capacity has been discharged. These phenomenon's are explained in the results of the NiCd battery electrical model.

4. Electrical Model of 8Ah NiCd Battery Cell

4.1. Charge Mode

The charge characteristics of NiCd batteries are affected by the current, time, temperature and other factors like the dynamics of charge process itself on the battery voltage. Increasing the charge current and lowering the charge temperature causes the battery voltage to rise. Charge generates heat, thus causing the battery temperature to rise. Charge efficiency will also vary according to the current, time and temperature [5,9].

$$V_{cell}^{ch} = V_o^{ch} + K_{ch} \cdot \frac{Q_{cell}^{ch}(t) + \int I^{ch} \cdot dt}{Q_n} + K_r \cdot I^{ch} + K_\tau \cdot (T_b - 20)\,(\mathrm{V}) \qquad (4)$$

The heat generated from cell during charge mode can expressed in the following form:

$$P_{cell}^{charg} = \begin{cases} (V_{cell}^{charg} - 1.44) \cdot I_{cell}^{ch}\,(W) & at \quad \int I_{cell}^{ch} \cdot dt \le Q_{cell}^{disch}\,(Ah) \\ 0.065\,(W) & at \quad \int I_{cell}^{ch} \cdot dt > Q_{cell}^{disch}\,(Ah), \end{cases} \qquad (5)$$

4.2. Discharge Mode

The discharge characteristics of NiCd batteries will vary according to the current, temperature and the dynamics of the discharge process also. The time of discharge depends on the efficiency of the battery, minimum discharge duration will be at EOL [5, 9].

$$V_{cell}^{disch} \cong V_o^{disch} - K_{dis} \cdot \frac{Q_{cell}^{disch}}{Q_n} - K_r \cdot I_{cell}^{disch} - K_\tau \cdot (T_b - 20)\,(V) \qquad (6)$$

Where:

$$V_o^{ch} \cong 1.34\mathrm{V}{:}1.36\mathrm{V}, \qquad V_o^{disch} \cong 1.41V$$

$$K_r \cong 0.006\,\Omega, \quad K_\tau \cong 0.0036\,(V * {}^oC^{-1}),$$

$$Q_n = 8\,Ah, \; , T_b - \; Bettery\; Temperature\; .$$

The heat generated from cell during discharge mode can expressed in the following form:

$$P_{cell}^{disch} \cong (1.461 - U_{cell}^{disch}) \cdot I_{cell}^{disch}\,(W) \qquad (7)$$

5. Results of NiCd battery electrical model analysis

A MatLab based GUI program is built to illustrate the NiCd electrical characteristics at different operation conditions. The battery nominal parameters like; number of stack cells, charge and discharge currents and internal resistance range are grouped together while the operation control parameters like; temperature and temperature coefficient, battery efficiency and operating period are grouped together. The program has the ability to simulate the NiCd battery operation at different conditions keeping the results in the same graph. To validate the introduced model, a comparison was done between the measured and simulated results at the same conditions; charge discharge current equals 3A. The measured results (Fig. 4) and simulated at the same parameters except the dynamics of temperature changes during test (Fig. 5) shows a similarity in both curves.

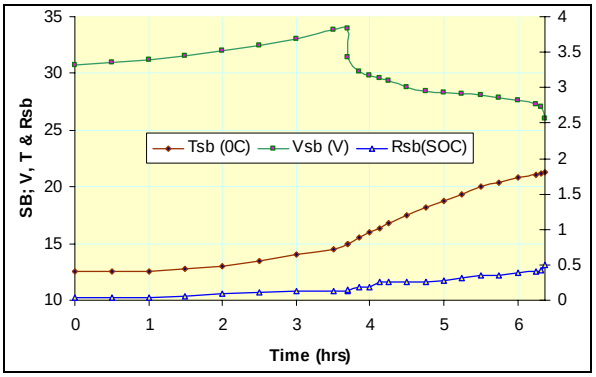

Fig. 4, Mesured values of NiCd 22 cells stack at 3A ch/dis current and 12.5 ^{O}C.

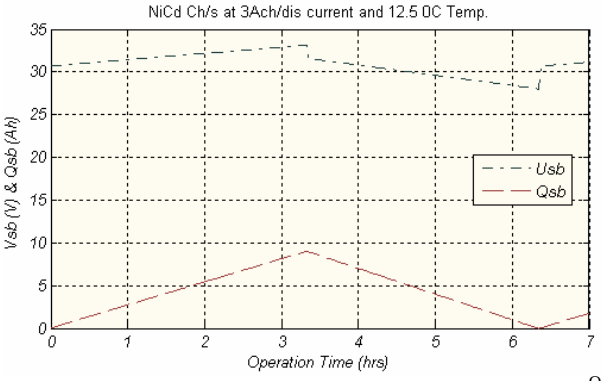

Fig. 5, GUI Model results at 3A ch/dis current & 12.5^{O}C

The battery performance is studied at different operation conditions that reflect the environment of operation in the LEO satellites. The battery stack voltage and capacity are studied at +5 ^{o}C : +35 ^{o}C temperature range and 80% & 90% battery efficiency (for new and nominal degraded one's). This test is done at 3A and 8A charging/discharging currents that simulate the nominal and loaded mode of the battery in-orbit operation. The results are shown in Fig.s (6-7).

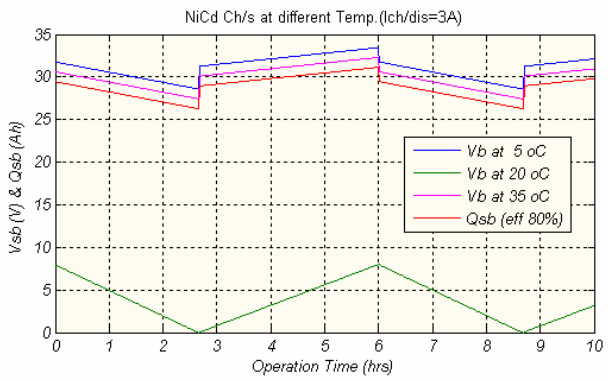

Fig. 6, NiCd battery characteristics at 3A ch/dis current and different temperature values while battery efficiency is 80%.

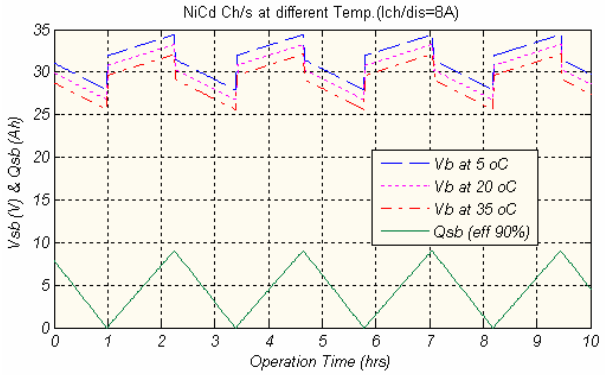

Fig. 7, NiCd battery characteristics at 8A ch/dis current and different temperature values at 90% battery efficiency.

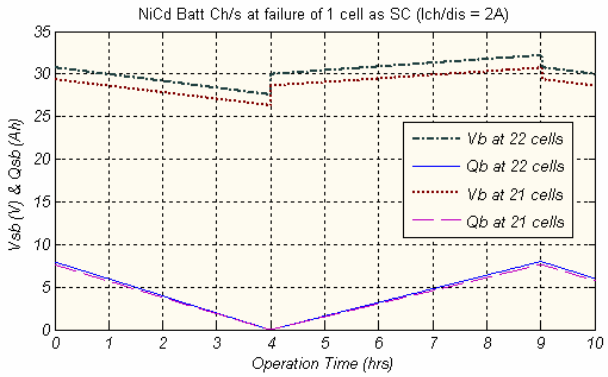

Fig. 8, Study the effect of one cell short circuit failure on the 22 NiCd battery stack performance.

Also the battery is simulated at 2A charging-discharging currents that represent the worst case of battery charging (average value) and satellite operation in standby mode as well as the off-nominal operation; failure of one cell. Results are shown in Fig. 8.

Figures 9, 10 illustrate the effect of changes in the internal resistance and temperature coefficient on the electrical battery performance.

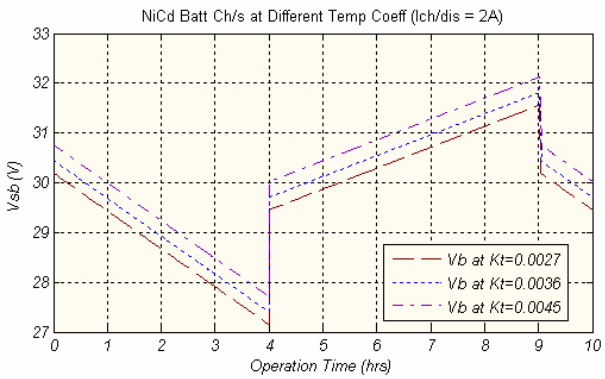

Fig. 9, Study the change of temperature coefficient on the NiCd battery stack performance

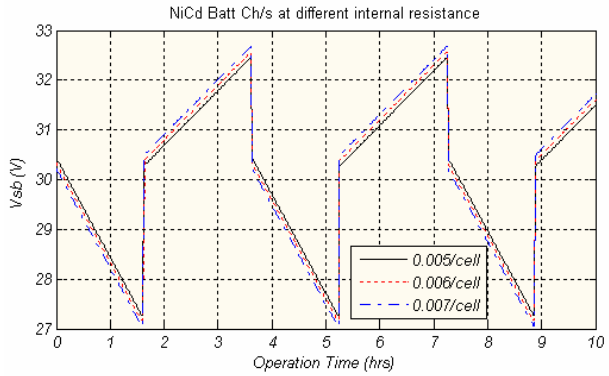

Fig. 10, Study the change of internal resistance on the NiCd battery stack performance

6. NiCd Battery Thermal Modelling

6.1. Survey of NiCd Batt. Thermal Control

NiCd cells were tested and analyzed to predict thermal behavior for battery designs that provide improved thermal performance by Gross and Malcolm [10]. Correlations have been developed to predict accurately cell heat generation and thermal joint resistance. A thermal model was derived and experimentally verified, then used to conduct a parametric study of the variables that determine the effectiveness of the packaging design. Cooling arrangement, materials, and heat generation uniformity were the variables.

Furthermore, a mathematical model for evaluating thermal behavior of batteries and electrochemical cells was developed by Lee [11]. In his paper, he reviewed

the methodology and applications of thermal modeling in various battery systems.

Newman and Tiedemann [12] developed a three-dimensional battery module in the shape of a block used to generate heat uniformly. The temperature rise as a function of time is worked out based on equations for heat conduction in solids. After appropriate nondimensionalization, the maximum temperature rise depends on the thermal aspect ratios (defined herein). By a superposition integral, the method can be extended to a time dependent heat generation rate, as appropriate for a driving profile.

A simplified overall enthalpy balance of a battery has been recently presented and discussed in terms of certain physical and thermophysical properties of batteries by Donahue [13]. These properties include enthalpy of the reaction(s) and internal resistance, overall heat transfer coefficient, and the heat capacity of the battery. The purpose of that work is to identify the operative components of NiCd batteries under various charging/discharging and heat transfer conditions.

Finally, Hwang et al. [14] discussed simple ways of determining charging efficiency and heat generation properties of a battery. These characteristics are described and applied to nickel hydrogen and NiCd cells.

6.2. Effect of Temperature

The performance of a NiCd cell depends on several factors such as operating temperature, charging–discharging rates, age of the cell, etc. The temperature at which the cell is discharged has a pronounced effect on its capacity and voltage characteristics. This is a result of the exothermicity of the discharging reactions in a NiCd cell. Lowering of the discharging temperature will result in a reduction of capacity as well as an increase in the slope of the discharging curve. The discharging profile varies for each battery system, design, and discharging rate, but generally best performance is obtained between 0 and 20°C. At higher temperatures, chemical deterioration may be rapid enough during the discharging to cause a loss of capacity [6]. The effect of temperature on the capacity and the average discharging voltage of a sealed NiCd cell is shown in Fig. 11, Fig. 12.

6.3. Cell Stack Thermal Model

The battery consists of 22 cells divided equally into two cell stacks. A cell stack is a configuration of several individual cells. Each cell stack is a configuration of eleven individual cells. The cell stacks would be connected electrically in parallel but thermally in series.

In order to model the thermal behavior of a cell stack, the energy balance should be defined around each of the cells in the stack. The model assumes that the temperature behavior of the cell stack is symmetric, and therefore only half of the cell stack is modeled. It is assumed that each cell is at a uniform temperature which is allowed to vary with time. Fig. 13 is a schematic showing the temperature profile of one half of the cell stacks with length L/2 for a stack of length L. The center of the stack is defined to be x = 0 and the outer face of the cell stack to be x = L/2.

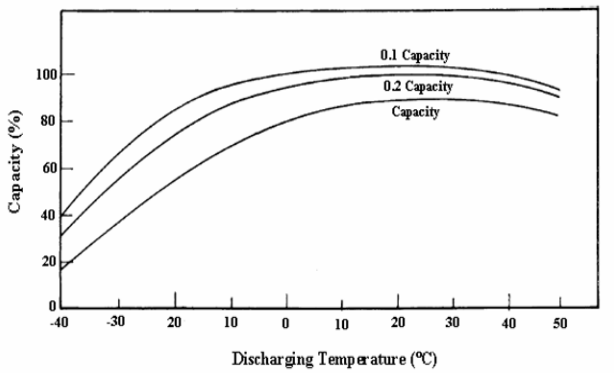

Fig. 11, The effect of temperature and discharge rate on the capacity after charging at 20 °C

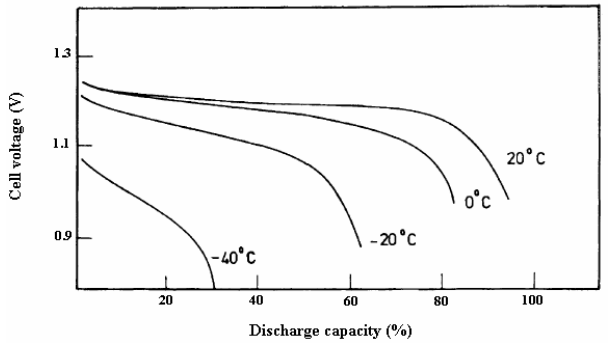

Fig. 12, The discharging voltage and available capacity as a function of temperature.

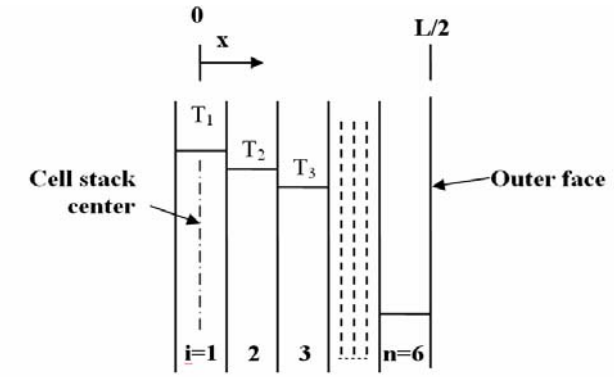

Fig. 13, Schematic of one half of one cell stacks used for energy balance

A fundamental feature of a simplified thermal analysis is the representation of the cells by just a few compact equations that are independent or connected by linearized coefficients. The ultimate simplicity in this regard is representing the cell by a single isothermal body i of thermal capacity $(mc_p)_i$ and radiating surface

area A_i^r, whose temperature T_i is indicative of the range expected for a whole region. To do this, the energy equation is reformulated by discarding the spatial derivatives and substituting for the term of heat generated by an expression that includes the heat generated in the cell per unit volume (q_i) less its net heat transfer to the surrounding by convection and to other cells by conduction.

Heat exchanges with other cells are included as a sum of products of temperature differences and modulating conductances. That is, if the heat transferred by convection to the ambient (at temperature T_j), and that by conduction to a cell at temperature (T_{i+1}) with conductance G_{cell} (W/K), then the energy equation reads

$$(mc_p)_i \frac{dT_i}{dt} = q_i - G_{cell}(T_i - T_{i+1}) - h(T_i - T_\infty) \quad (8)$$

For i=1. The temperature will be higher at the center of the cell stack (Fig. 13) than the temperature at the edges and due to symmetry assumed. This makes the input term for cell 1 falls out of Equation. (8). For i=2 through n-1:

$$(mc_p)_i \frac{dT_i}{dt} = q_i + G_{cell}(T_{i-1} - T_i) - G_{cell}(T_i - T_{i+1}) - h(T_i - T_\infty) \quad (9)$$

and for i=n:

$$(mc_p)_i \frac{dT_i}{dt} = q_i + G_{cell}(T_{i-1} - T_i) - h(T_i - T_\infty) \quad (10)$$

With initial condition $T(0)= T_o$ for all cells, the rate of heat generated in cell i, Q_i, is calculated from Equation's. (11) and (12). For simplicity, according to the analysis of Montalenti and Stangerup [15], the heat generation rate within a cell is assumed to be uniform; hence the heat generation rate per unit volume of the cell can be written as:

- During discharging

$$q = I\left(E_{oc} - E - T\frac{dE_{oc}}{dT}\right) \quad (11)$$

- During charging,

$$q = I\left[\left(E - E_{oc} - T\frac{dE_{oc}}{dT}\right)\eta\right] \quad (12)$$

where:

I	Cell current
E_{oc}	Cell open circuit voltage
E	Cell voltage,
T	the cell temperature, K
η	charging efficiency

It should be noted that battery efficiency η appears in the charge equation since that all the power is not converted into chemical energy.

Macdonald and Challingsworth, [16] had shown that the open circuit voltage can be considered constant over the optimum operating temperature range of NiCd cells (0-20°C). Vaidyanathan and Rao [17] calculated the open circuit voltage by measuring the heat rates during charging and discharging processes. The experimental value was 1.461 V. Knowledge of the open circuit voltage allows calculation of the total cell heat generation over a wide range of currents requiring only knowledge of the cell voltage profile. With both I, η and E prescribed, the heat generation rate per unit volume in Equation's. (11) and (12) can be determined.

Fig. 14 shows the values of both measured charging and discharging voltage plotted against time for the battery under test. The heat generation rate as a function of time is given in the same Fig. for the same charging and discharging conditions. Fig.14 demonstrates that the cell is endothermic during most of the charging period followed by exothermic reaction as the cell nears full charging.

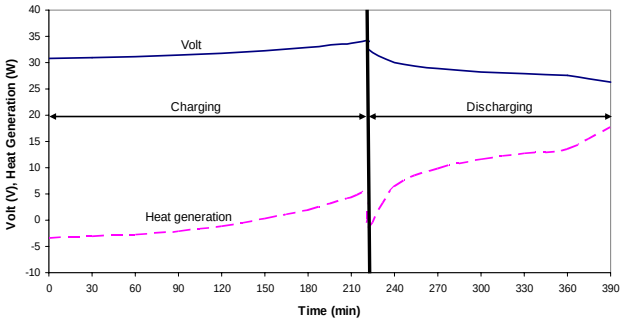

Fig. 14, Measured cell voltage during ch/disch cycle and calculated heat generation

The discharging is exothermic during the entire discharging period. The heat generation rate increases dramatically near the end of discharging because of the decrease of the discharging voltage as shown in Fig. 14.

6.4. Temperature Profiles during Charging and Discharging states

Fig. 15 shows calculated and measured temperature profiles in half of the cell stack as function of time for three different values of current during discharging. For I=3A, the calculated and measured temperatures show good agreement.

The temperature difference between them is about 1 °C. This proves the validity of the thermal model developed to predict the temperature profile in the cell stack. In addition, this model can be used to predict the temperature profile in the cell stack for different values of current. For I=5A, the cell stack model predicts a temperature about 29 °C at the end of discharging process while the same model predicts 40 °C for I=8A. The three calculated temperature curves deviate as long

as the discharging process takes place until they reach their maximum deviation at the end of the process.

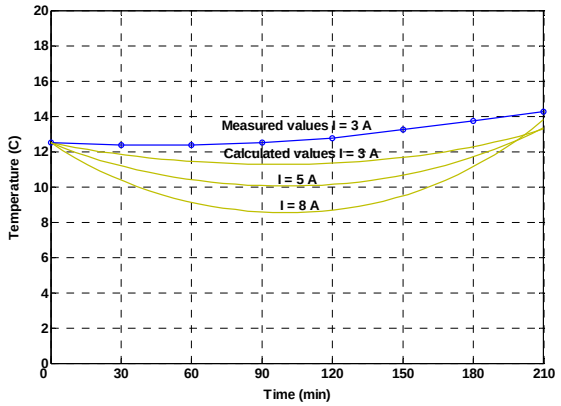

Fig. 15, Measured and calculated temperature as a function of time during discharging (T_∞=12.5 °C).

Fig. 16 shows the calculated and measured temperature profiles of one half of the cell stack during charging. For early times, the temperature decreases in the cell stack due to the endothermic reaction inside the cells. The results show that the average temperature decreases slightly till half of the charging time. As the charging process proceeds, the temperature increases due to the transition from an endothermic reaction to an exothermic reaction. At the end of charging process, the temperature reaches about 13 °C for the three values of charging currents. The temperature difference between the measured and calculated temperatures for I=3A reaches its maximum value -about 2 °C- after three hours of charging.

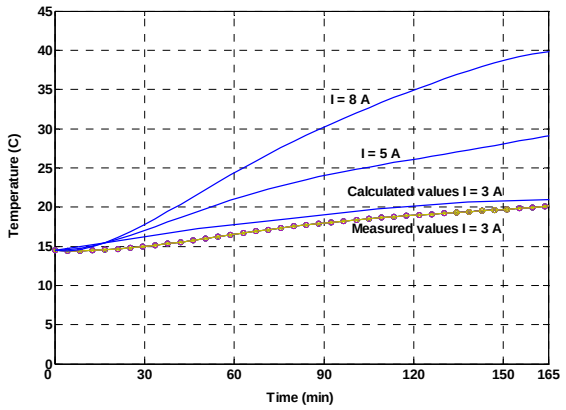

Fig. 16, Measured and calculated temperature as a function of time during charging (T_∞=12.5 °C).

7. Conclusion

The chemical, electrical and thermal characteristics of an 8Ah NiCd battery stack of 22 cells connected in series are illustrated in this paper. The electrical and thermal model of the battery are introduced and analyzed. A MatLab based Graphical User Interface program is built to simulate the NiCd battery under study. The program has the ability to simulate the NiCd battery operation at different conditions keeping the results in the same graph. The results show that a convergence between the simulated and measured values of both electrical and thermal models. The discussion of results is detailed presented in sections 4-6 in this paper.

8. References

1. Cyril Annarella, et.al, "A Space Systems Design Proposal for ASE396 - Space Systems Design", University of Texas at Austin, December 7, 1994.
2. Wertz, J. and Larson, W., Eds., Space Mission Analysis and Design. Boston, Kluwer Academic Publishers, 1991.
3. ECSS Secretariat, ESA—ESTEC, Requirements & Standards Division, "Space engineering, Electrical and electronic", ESA Publications Division, ESTEC, P.O. Box 299, 2200 AG Noordwijk, The Netherlands, 4 October 1999, ISSN: 1028-396X
4. Carl B. Faclon, “Teemperature termination and the thermal characteristics of NiCd and NiMH Batteries”, Integrated Circuit systems, Inc. 2435 Boulevard of the Generals Vally Forge, PA 19468.
5. D.G. Belov, et.al, “Electric Power Supply for Ocean Satellite”, sixth European Space Power Conference, Porto, Portugal, 6-10 May 2002 (ESA SP –502, May 2002).
6. A.K. Shuklaa,*, S. Venugopalanb, B. Hariprakash, “Nickel-based rechargeable batteries”, Journal of Power Sources 100 (2001) 125–148
7. Chester Simpson, “Characteristics of Rechargeable Batteries” *National Semiconductor*
8. RAE Systems, "Proper care of NiCd battery back", www.raesystem.com , TN-145
9. Matsushita Battery Industrial Co., Ltd, “Panasonic NiCd battery Handbook”, Augest 1998.
10. Gross, S. and Malcolm, J., “Thermal Considerations of Sealed Nickel-Cadmium Batteries”, Proceedings of the Eighth International Symposium on High Performance Capillary Electrophoresis, pp. 257-275, Brighton, Sussex, England, 1973.
11. Lee, J., “Battery Thermal Modeling - The Methodology and Applications”, Symposium on Electrochemical and Thermal Modeling of Battery, Fuel Cell, and Photo energy Conversion Systems, pp. 206-215,San Diego, CA, 1986.
12. Newman, J. and Tiedemann, W., “Temperature Rise in a Battery Module with Constant Heat Generation”, Journal of Electrochemical Society, Vol. 142, pp. 1054-1057, April, 1995.
13. Donahue, F. M., “Thermal Characteristics of Batteries”, Annual Battery Conference on

Applications and Advances, 14th, California State University, 1999.
14. Hwang, W., Matsumoto, J., and Prater, A., "Determination of Thermal and Charging Characteristics of Satellite Batteries", Proceedings, 33rd Intersociety Energy Conversion Engineering Conference, Colorado Springs, pp. 265-268, 1998.
15. Montalenti, P. and Stangerup, P., "Thermal simulation of NiCd Batteries for Spacecraft", Journal of Power Sources, 2, pp. 147-162, 1977.
16. Macdonald, D. D. and Challingsworth, M. L., "Thermodynamics of Nickel-Cadmium and Nickel-Hydrogen Batteries", Journal of Electrochemical Society, 140, pp. 606-609, 1993.
17. Vaidyanathan, H. and Rao, G. M., "Electrode Properties and Heat Generation Rate in Ni-cd, Ni-H_2, and Ni-MH Cells", Proceedings, 31st Intersociety Energy Conversion Engineering Conference, Vol. 1, pp. 83-86, 1996.

Dr. Mohamed Bayoumy A. Zahran (M. Zahran), was born in Egypt, Received his B.Sc from Kima High Institute of Technology, M.Sc in 1993 and Ph.D. in 1999 from Cairo University, Faculty of Engineering, Electrical Power and Machines Dept. He is Researcher in the Electronics Research Institute, Photovoltaic Cells Dept. His experience is mainly in the field of renewable energy sources, systems design, management and control. Currently is employed by National Authority for Remote Sensing and Space Science (NARSS). He is a member in the Egyptian Space Program in the Satellite EPS Dept.

Ayman A. Megahed, was born in 1976 in Egypt and graduated from the Faculty of Engineering, Mechanical Power Department - Cairo University in 1999. He received his M.Sc. in 2006 from Cairo University, Faculty of Engineering, Mechanical Power Dept. He is a Research Assistant in National Authority for Remote Sensing and Space Science (NARSS), Cairo Egypt, Space Dept. since March 2001. His experience is mainly in the field of satellite thermal control.